# Nuclear receptor PPARγ-regulated monoacylglycerol *O*-acyltransferase 1 (MGAT1) expression is responsible for the lipid accumulation in diet-induced hepatic steatosis

Yoo Jeong Lee[a,b], Eun Hee Ko[a,b], Ji Eun Kim[a], Eunha Kim[a], Hyemin Lee[a,c], Hyeonjin Choi[a,b], Jung Hwan Yu[a,b], Hyo Jung Kim[a], Je-Kyung Seong[d], Kyung-Sup Kim[a,b], and Jae-woo Kim[a,b,c,1]

[a]Department of Biochemistry and Molecular Biology, Integrated Genomic Research Center for Metabolic Regulation, Institute of Genetic Science, Yonsei University College of Medicine, Seoul 120-752, Korea; [b]Brain Korea 21 Project for Medical Science, Yonsei University, Seoul 120-752, Korea; [c]Department of Integrated OMICS for Biomedical Sciences, World Class University (WCU) Program of Graduate School, Yonsei University, Seoul 120-749, Korea; and [d]Department of Anatomy and Cell Biology, College of Veterinary Medicine and Research Institute for Veterinary Science, Seoul National University, Seoul 151-742, Korea

Edited by Evan D. Rosen, Beth Israel Deaconess Medical Center, Boston, MA, and accepted by the Editorial Board July 10, 2012 (received for review February 23, 2012)

**Recently, hepatic peroxisome proliferator-activated receptor (PPAR)γ has been implicated in hepatic lipid accumulation. We found that the C3H mouse strain does not express PPARγ in the liver and, when subject to a high-fat diet, is resistant to hepatic steatosis, compared with C57BL/6 (B6) mice. Adenoviral PPARγ2 injection into B6 and C3H mice caused hepatic steatosis, and microarray analysis demonstrated that hepatic PPARγ2 expression is associated with genes involved in fatty acid transport and the triglyceride synthesis pathway. In particular, hepatic PPARγ2 expression significantly increased the expression of monoacylglycerol *O*-acyltransferase 1 (MGAT1). Promoter analysis by luciferase assay and electrophoretic mobility shift assay as well as chromatin immunoprecipitation assay revealed that PPARγ2 directly regulates the MGAT1 promoter activity. The MGAT1 overexpression in cultured hepatocytes enhanced triglyceride synthesis without an increase of PPARγ expression. Importantly, knockdown of MGAT1 in the liver significantly reduced hepatic steatosis in 12-wk-old high-fat–fed mice as well as ob/ob mice, accompanied by weight loss and improved glucose tolerance. These results suggest that the MGAT1 pathway induced by hepatic PPARγ is critically important in the development of hepatic steatosis during diet-induced obesity.**

nonalcoholic fatty liver disease | adenoviral expression | SREBP1c | ChREBP | TLR4

Metabolic syndrome is characterized by a combination of central obesity, dyslipidemia, hypertension, hepatic steatosis, and abnormal glucose tolerance (1). Although the exact etiology of metabolic syndrome has not yet been defined, most patients have some degree of insulin resistance, which is considered an underlying mechanism in development of a combination of disorders (2). Metabolic syndrome is closely associated with nonalcoholic fatty liver disease, characterized by an increased hepatic lipid content (i.e., hepatic steatosis) (3). It is widely believed that an excessive amount of intrahepatic triglyceride (TG) results from an imbalance between complex interactions of metabolic events.

To date, two major transcription factors, sterol regulatory element-binding protein 1c (SREBP1c) and carbohydrate responsive element-binding protein (ChREBP), have been implicated in fatty liver formation (4). SREBP1c, stimulated by insulin during the postprandial state, regulates a cluster of genes involved in glycolysis and fatty acid synthesis, thereby inducing conversion of excess dietary glucose into TG in the liver. ChREBP also regulates a similar pathway through liver-type pyruvate kinase expression as well as lipogenic genes (5). However, many studies have demonstrated that these two transcription factors are essentially associated with regulating de novo fatty acid synthesis from the carbohydrate sources of a diet (4). It is still uncertain whether these two transcription factors are involved in high-fat–induced severe hepatic steatosis in a living animal.

In contrast to these two transcription factors, peroxisome proliferator-activated receptor γ (PPARγ) was recently described as involved in hepatic steatosis. Generally, PPARγ is expressed at a low level in human and mouse liver, ∼10–30% of that in adipose tissue (6). However, there is emerging evidence that hepatic PPARγ plays an important role in metabolic syndrome. First, it was reported that liver PPARγ2 was significantly up-regulated in a rodent model of obesity, indicating that PPARγ plays an important role in fatty liver formation (7, 8). In this regard, it was not surprising that inhibition of retinoid X receptor (RXR) and PPARγ ameliorated diet-induced obesity (DIO) and diabetes (9). Accordingly, liver-specific disruption of *PPARγ* in ob/ob mice improves fatty liver (10). This deficiency of hepatic PPARγ in ob/ob mice, however, showed further aggravation of diabetes accompanied by decreased insulin sensitivity in muscle and fat (10). Therefore, although the relationship between hepatic steatosis and systemic insulin resistance remains to be further defined, these results strongly suggest that the PPARγ signaling pathway is involved in diet-induced liver steatosis, and lipid accumulation may be prevented by down-regulation of the PPARγ gene in the hepatocytes.

The molecular mechanism of how PPARγ induces hepatic steatosis is not fully understood. When the hepatocytes aberrantly express PPARγ at a high level, several adipocyte-specific genes and lipogenesis-related genes are induced, such as adipsin, adiponectin, aP2/422, and fat-specific gene 27 (FSP27) (11). Other reports showed that adipose differentiation-related protein (ADRP) was up-regulated in PPARγ-overexpressing hepatocytes (12). These results suggest that hepatic PPARγ enhances lipid accumulation in liver mainly through the up-regulation of adipogenic genes; however, it remains to be seen whether PPARγ directly regulates genes involved in hepatic lipid metabolism, including the TG synthesis pathway.

In this study, we found that C3H mice do not express PPARγ in the liver and are resistant to hepatic steatosis when fed a high-fat diet (HFD). Using the advantage of this animal model, we found that monoacylglycerol *O*-acyltransferase 1 (MGAT1) is directly regulated by PPARγ and plays a role in regulating the pathway leading to incorporation of fatty acid into TG. Our data suggest that increased PPARγ and MGAT1 activity during a HFD plays

Author contributions: Y.J.L., E.H.K., and J.-w.K. designed research; Y.J.L., E.H.K., J.E.K., E.K., H.L., H.C., J.H.Y., and J.-w.K. performed research; J.-K.S. contributed new reagents/analytic tools; Y.J.L., E.H.K., H.J.K., J.-K.S., K.-S.K., and J.-w.K. analyzed data; and Y.J.L. and J.-w.K. wrote the paper.

The authors declare no conflict of interest.

This article is a PNAS Direct Submission. E.D.R. is a guest editor invited by the Editorial Board.

[1]To whom correspondence should be addressed. E-mail: japol13@yuhs.ac.

This article contains supporting information online at www.pnas.org/lookup/suppl/doi:10.1073/pnas.1203218109/-/DCSupplemental.

a major role in developing hepatic steatosis by regulating fatty acid transport and the TG incorporation pathway.

## Results

**C3H Mice Do Not Express PPARγ in Liver and Are Resistant to Hepatic Steatosis During a HFD.** C57BL/6 (B6) mice are largely used in metabolic disease research because they develop severe obesity and diabetes after several weeks of a HFD (13). Compared with B6 mice, we examined the metabolic profile of C3H mice under a normal chow diet (CD) or a HFD. High-fat–fed B6 mice showed significantly higher final body weight and cumulative body weight gain compared with CD-fed mice (Fig. 1*A*). Importantly, HFD-fed C3H mice also showed significantly higher final body weight, indicating that these mice should be considered a DIO-prone strain. However, C3H mice showed normal glucose tolerance despite a high degree of obesity (Fig. 1*B*). In addition, plasma LDL cholesterol did not rise to a significant level in C3H compared with B6 mice when both were fed the HFD (Table S1), suggesting that C3H mice might be a mouse strain that represents less clinically harmful human obesity. Whereas the liver weight of HFD-fed B6 mice was significantly higher than that of CD-fed B6 mice, there was no difference in liver weight between HFD-fed and CD-fed C3H mice (Fig. S1*A*). Both mouse strains had markedly increased fat pads after HFD, explaining the similar weight gain. It should be noted that HFD-fed B6 mice had larger epididymal fat pads compared with C3H mice, whereas C3H mice had larger s.c. fat pads (Fig. S1*B*). This result is noteworthy because the visceral fat content rather than s.c. fat content is known to contribute to the development of metabolic syndrome. As shown by the increased liver weight, severe hepatic steatosis was observed with increased liver TG level in HFD-fed B6 compared with HFD-fed C3H mice (Fig. 1 *C* and *D*).

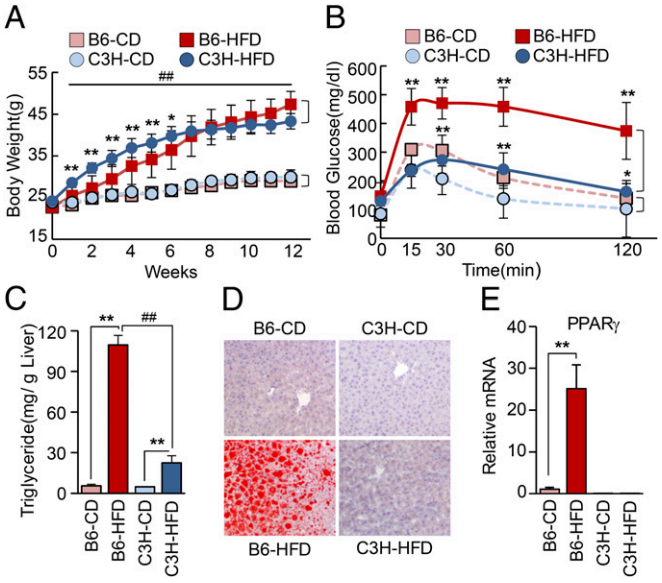


**Fig. 1.** Comparison of metabolic response to high-fat diet between B6 and C3H mice. (*A*) Body weight changes of B6 and C3H mice fed a CD or a HFD. $*P < 0.05$, $**P < 0.01$ relative to diet-matched B6 and C3H mice, and $^{\#\#}P < 0.01$ relative to corresponding CD controls. (*B*) Glucose tolerance test in B6 and C3H mice fed CD or HFD. $*P < 0.05$, $**P < 0.01$ for B6 vs. C3H with CD or HFD, respectively. (*C*) TG content in the livers of B6 and C3H mice. $**P < 0.01$ relative to corresponding CD controls, and $^{\#\#}P < 0.01$ between HFD groups. Data in *A*–*C* represent the mean ± SD and were analyzed by two-way ANOVA (CD and HFD: $n = 8$ and 9, respectively). (*D*) Increased lipid deposition, as indicated by oil-Red-O lipid staining in liver sections from mice in the CD or HFD groups at 12 wk. (*E*) Hepatic PPARγ2 mRNA expression measured by real-time PCR in liver from B6 and C3H mice fed CD or HFD at 12 wk. $**P < 0.01$. Data represent the mean ± SD.

Strikingly, liver PPARγ (mainly PPARγ2) mRNA and protein were markedly elevated in B6 but not in C3H mice after 12 wk of HFD (Fig. 1*E* and Fig. S1 *C* and *D*). In addition, PPARγ binding activity in EMSA experiments showed the same pattern as that of the mRNA changes (Fig. S1*E*). The near absence of both PPARγ1 and PPARγ2 expression in the liver of C3H mice even under CD should be noted (Fig. 1*E*). Importantly, white adipose tissue of C3H mice expressed PPARγ as much as that of B6 mice, indicating that the phenomenon we observe in this study is liver-specific (Fig. S1*C*). Meanwhile, previous reports indicated that a loss-of-function mutation in the Toll-like receptor (TLR4) in C3H/HeJ mice prevents diet-induced obesity and insulin resistance (14, 15). However, we found that both the C3H/HeN mice (carrying wild-type TLR4) and the C3H/HeJ mice (carrying mutated TLR4) did not show the difference in hepatic steatosis in response to 12-wk HFD (Fig. S2). Moreover, both C3H/HeN and C3H/HeJ mice showed similar patterns of PPARγ expression in liver (Fig. S2*G*), suggesting that mice lacking hepatic PPARγ expression may be protected against the development of hepatic steatosis and glucose intolerance under HFD conditions, independent of TLR4 function. It is not clear why C3H mice do not express PPARγ in the liver, but the epigenetic control may partly contribute to this phenomenon. Although methylation status in the *PPARγ1* and the *PPARγ2* promoter did not show any differences between livers of B6 and C3H mice (Fig. S3*A*), increased H3 acetylation in the promoter regions of *PPARγ1* and *PPARγ2* of B6 mice compared with C3H mice was observed (Fig. S3*B*).

**Hepatic PPARγ Regulates Expression of Genes Related to Fatty Acid Transport and TG Synthesis.** To verify the functional significance of PPARγ in the fatty liver in vivo, we injected adenoviral PPARγ2 (Ad-PPARγ2) into B6 and C3H mice via tail veins, resulting in overexpression of PPARγ2. Ectopic expression of hepatic PPARγ2 was verified by real-time PCR as well as Western blot analysis (Fig. 2 *A* and *B*). As expected, PPARγ2 overexpression resulted in a marked induction of several PPARγ targets, including aP2/422, CD36, and ADRP (Fig. 2 *A* and *B*). Consistently, Ad-PPARγ2 mice showed higher levels of hepatic TG than control Ad-GFP mice (Fig. 2*C*). Histological analysis of the liver from Ad-GFP or Ad-PPARγ2 mice revealed the presence of numerous fat droplets in the Ad-PPARγ2–injected B6 and C3H mice (Fig. 2*D*). It should be noted that the PPARγ expression after adenovirus injection into B6 mice was 1.8-fold higher compared with that in C3H mice (Fig. 2 *A* and *B*). The reason for the difference in the level of overexpression attained in each strain remains uncertain, but the degree of hepatic steatosis in B6 and C3H mice (Fig. 2 *C* and *D*) was correlated with the degree of PPARγ expression.

These findings were confirmed in vitro, using primary hepatocytes from B6 and C3H mice with PPARγ2 overexpression. When Ad-PPARγ2 was added to primary hepatocytes, aP2/422, CD36, and FSP27 were expressed both in B6 and in C3H hepatocytes, which was further enhanced with a PPARγ agonist, rosiglitazone treatment (Fig. S4 *A* and *B*). Consistent with previous findings, the TG level significantly increased in primary hepatocytes with Ad-PPARγ2 virus compared with Ad-GFP virus (Fig. S4*C*). Indeed, the TG level increased further by the addition of palmitate, suggesting that PPARγ2 is involved in the fatty acid incorporation pathway. As previously reported (12), alpha mouse liver (AML)-12 hepatocytes infected by Ad-PPARγ2 virus also demonstrated that ADRP coats lipid droplets in PPARγ2-expressing hepatocytes at higher levels compared with levels observed in control hepatocytes (Fig. S4*D*), supporting a critical role of PPARγ in hepatic TG synthesis.

To analyze the profile of PPARγ-regulated genes in steatotic liver, we performed two sets of microarray experiments using RNAs from B6 vs. C3H with CD or HFD and B6 and C3H with or without Ad-PPARγ2 injection. Data in Table S2 and Fig. S5*A* indicate that hepatic PPARγ induces genes mainly involved in cellular uptake and TG incorporation of fatty acids. It is noteworthy that C3H liver expressed a considerable amount of SREBP1c in response to HFD

CELL BIOLOGY

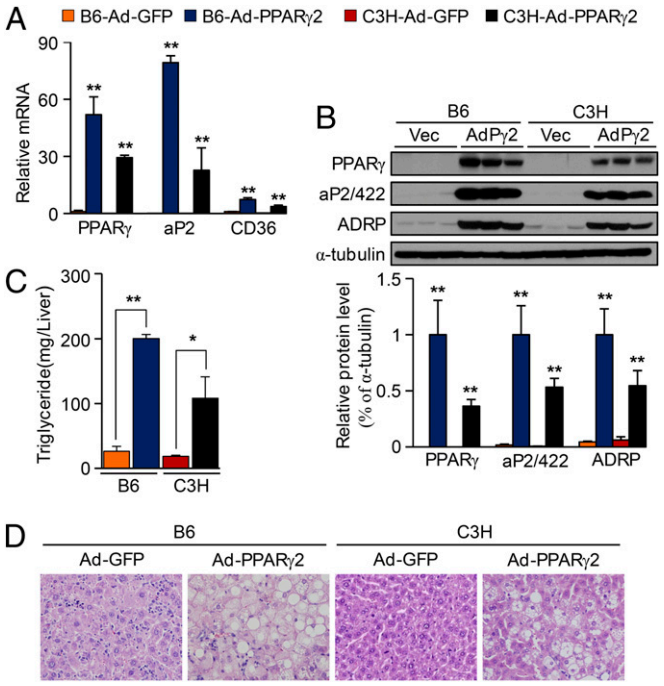


**Fig. 2.** Adenoviral expression of PPARγ resulted in hepatic steatosis in vivo in B6 and C3H mice. Mice at 7 wk old were injected with Ad-PPARγ2 or an Ad-GFP, fed with CD for 1 wk, and then killed. (*A*) Real-time PCR analysis of PPARγ2 and its target genes in liver of B6 and C3H mice. (*B*) Total protein was isolated from individual livers of Ad-GFP and Ad-PPARγ2 mice. (*Upper*) Representative Western blots; (*Lower*) densitometry results. (*C*) Hepatic TG content determined in B6 and C3H mice infected with Ad-GFP or Ad-PPARγ2. ($n$ = 4.) (*D*) H&E staining performed on liver sections from mice as shown. Data in *A*–*C* represent the mean ± SD. $^{*}P < 0.05$, $^{**}P < 0.01$.

(Fig. S5*A*), and therefore there is no remarkable difference of lipogenic genes such as *ACL*, *ACC*, and *FAS* between B6 and C3H mice. To study how PPARγ overexpression affects fatty acid transport, we adopted real-time quantification of fatty acid uptake, using a fluorescence assay (16). As shown in Fig. S5*B*, adenoviral overexpression of PPARγ2 resulted in increased fatty acid transport into the hepatocytes isolated both from B6 and from C3H mice. Baseline fatty acid transport was also higher in B6 mice than in C3H mice. This phenomenon was reversed by the addition of GW9662, a synthetic PPARγ antagonist. Therefore, it is concluded that at least one mechanism related to PPARγ activity in hepatic steatosis is involved in this increase of fatty acid transport. This activity likely occurs through the induction of aP2/422 and CD36.

**Hepatic PPARγ Directly Regulates the Expression of MGAT1.** Interestingly, PPARγ2 overexpression caused a marked induction of MGAT1 (Table S2 and Fig. S5*A*). This enzyme is involved in incorporation of fatty acids into TG (17, 18), providing an alternative pathway for TG synthesis that has also been demonstrated in 1-acylglycerol-3-phosphate *O*-acyltransferase 2 (AGPAT2) knockout mice (18). Indeed, MGAT1 was induced both by HFD-induced steatosis and by Ad-PPARγ2 overexpression (Fig. 3*A*). Furthermore, knockdown of PPARγ using siRNA in primary hepatocytes showed marked reduction of MGAT1 expression (Fig. 3*B*). This result opens the possibility that PPARγ activates the MGAT pathway, leading to accelerated TG synthesis from excessive amounts of fatty acids, and MGAT1 is one of the target genes regulated by PPARγ. To access this hypothesis, we analyzed ~2 kb of the MGAT1 promoter sequence. Computer analysis of the mouse MGAT1 promoter identified four putative PPAR-responsive elements (PPREs) within this region, and luciferase assays showed marked activation of MGAT1 promoter by PPARγ expression in 293T cells as well as primary hepatocytes (Fig. 3 *C* and *D*). Of these, −194 and −51 regions strongly bound PPARγ in EMSA experiments (Fig. 3*E* and Fig. S6*A*), demonstrating that MGAT1 is a direct target gene of PPARγ. This result was further confirmed by deletion and mutation analysis of the promoter. As shown in Fig. S6 *A*–*C*, deletion or mutation of −194 and −51 almost completely abolished the promoter activity driven by PPARγ. It was also confirmed that the mutation of −194 or −51 disrupted the PPARγ binding by EMSA experiment (Fig. S6*D*). Finally, a chromatin immunoprecipitation (ChIP) assay was carried out to confirm the in vivo binding of PPARγ to the MGAT1 promoter, which was greatly enhanced in HFD-fed and ob/ob mice (Fig. 3*F*). Taken together, it is concluded that PPARγ directly regulates the MGAT1 promoter activity by binding to both −194 and −51 regions.

**MGAT1 Plays an Important Role in the Hepatic Steatosis Induced by HFD and PPARγ.** The liver has the ability to accumulate lipids in a healthy subject, mainly by the classical glycerol 3-phosphate pathway. A previous study demonstrated that the MGAT pathway is merely involved in TG biosynthesis in the normal liver because of the very low expression and activity of MGAT1 (18). Our data also show that MGAT1 was not expressed under a normal diet in B6 and C3H mice (Fig. 3*A*). To determine the functional significance of the MGAT1 pathway in steatotic liver, we generated an adenoviral MGAT1-FLAG expression vector, and the adenovirus was added to AML-12 cells. These cells were subjected to immunocytochemistry using anti-ADRP antibody, which localizes to the lipid droplet. As shown in Fig. 4 *A*–*C*,

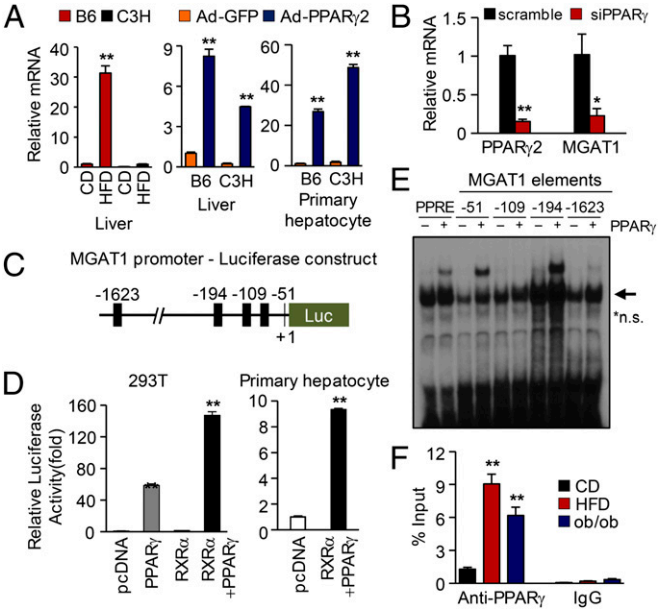


**Fig. 3.** PPARγ directly regulates MGAT1 promoter activity. (*A*) MGAT1 mRNA expression in livers of B6 and C3H mice on a HFD or with Ad-PPARγ2 overexpression or in primary hepatocytes from B6 and C3H mice with PPARγ overexpression. (*B*) PPARγ knockdown in primary hepatocytes isolated from B6 mice resulted in marked reduction of MGAT1 expression, measured by real-time PCR. (*C*) The luciferase construct of the 5′-flanking region of the mouse MGAT1 gene, containing putative PPREs (black squares). (*D*) Luciferase assay using mouse MGAT1 promoter. The promoter activity was shown by relative luciferase activity, with overexpression of RXRα and/or PPARγ2 in either 293T cells or mouse primary hepatocytes. (*E*) EMSA experiment of four putative PPREs on the mouse MGAT1 promoter. The oligonucleotides shown in Fig. S6*A* were labeled and incubated with TNT-translated mouse PPARγ and RXRα proteins (*n.s., nonspecific bands). (*F*) ChIP assay using anti-PPARγ antibody. The proximal promoter region of MGAT1 promoter was amplified by real-time PCR. Data in *A*, *B*, *D*, and *F* represent the mean ± SD. $^{*}P < 0.05$*, $^{**}P < 0.01$.

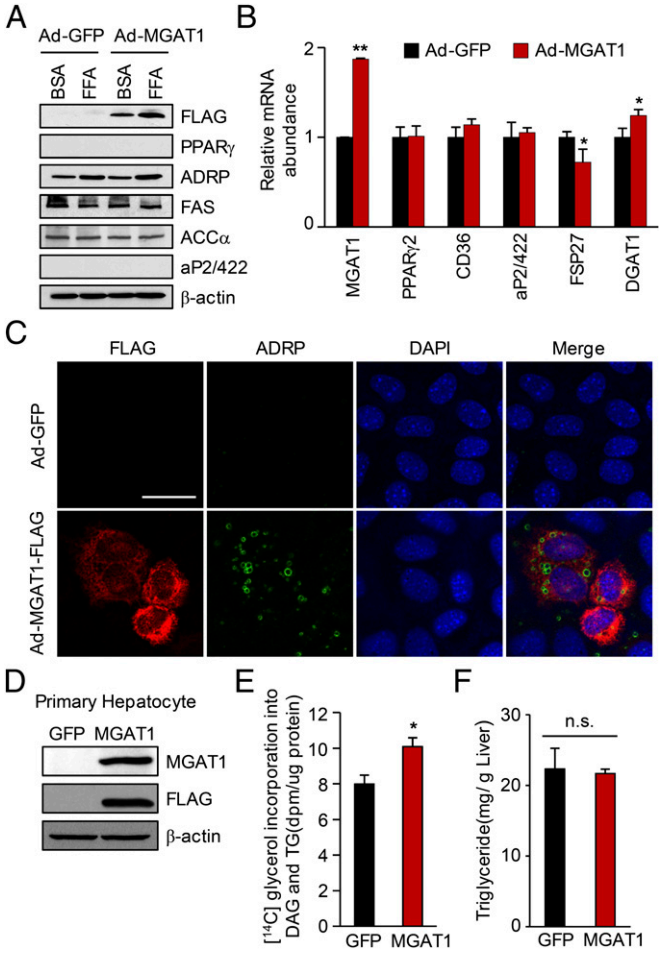


**Fig. 4.** MGAT1 overexpression resulted in increased lipid accumulation in hepatocytes. (*A–C*) AML-12 cells were infected with adenovirus expressing MGAT1-FLAG or GFP as a control as indicated. After 2 d, cells were incubated with palmitate (0.5 mM final concentration) in 1% FBS-DMEM for 24 h. (*A*) Total cell lysates were analyzed by Western blot analysis with the indicated antibodies. (*B*) Total RNA was prepared from the cells and analyzed by real-time PCR. (*C*) Double-immunofluorescence staining for FLAG (red) and ADRP (green) of AML-12 cells. The individual fluorescence values of each antibody were observed with a confocal microscope. (Scale bar, 50 μm.) (*D* and *E*) Primary mouse hepatocytes were isolated and infected with Ad-MGAT1-FLAG or GFP, and cells were labeled with [$^{14}$C]glycerol for 4 h. (*D*) Western blot showing MGAT1 overexpression. (*E*) The [$^{14}$C]glycerol incorporation into TG and DAG was counted after TLC of the lipid sample. (*F*) Adenoviral expression of MGAT1 in mice was not sufficient to increase hepatic TG content. Mice were injected with adenovirus, fed with CD for 1 wk, and then killed. Data in *B* and *E* represent the mean ± SD. $^*P < 0.05$, $^{**}P < 0.01$; n.s., not significant.

MGAT1 overexpression resulted in increased lipid accumulation in the cells with no increase of other PPARγ-regulated genes. We also analyzed the effect of MGAT1 overexpression in primary mouse hepatocyte. To analyze the lipid accumulation by MGAT1 overexpression in primary hepatocytes, we adopted the measurement of triglyceride synthesis, using [$^{14}$C]glycerol (18). As shown in Fig. 4 *D* and *E*, MGAT1 overexpression in primary hepatocytes resulted in significantly increased TG and DAG de novo synthesis. However, injection of adenovirus expressing MGAT1-FLAG into mice failed to increase hepatic TG contents within 1 wk of viral injection (Fig. 4*F*), suggesting that MGAT1 alone is not sufficient to produce hepatic steatosis in vivo. It is likely that other PPARγ-regulated genes, such as aP2/422, CD36, and Fsp27, are required for the enhanced TG synthesis in mice.

To directly demonstrate the role of MGAT1 expression in PPARγ-induced hepatic steatosis, we generated adenovirus expressing small hairpin RNA targeting MGAT1 mRNA. We first selected siRNA target sites that efficiently suppressed the MGAT1 expression among siRNAs samples and then produced two different Ad-shMGAT1 viruses. To test the effect of MGAT1 knockdown, either adenoviral sh-MGAT1s or a control vector was injected via tail vein along with an Ad-PPARγ2 virus. As shown in Fig. 5, the PPARγ-dependent elevation of lipid accumulation was dramatically blunted by knockdown MGAT1, indicating that MGAT1 plays a critical role in the PPARγ-induced lipid accumulation pathway in liver. Next, we investigated whether acute reduction of MGAT1 in mice with HFD-induced hepatic steatosis could affect the amount of TG content in the liver. Six-week-old B6 mice were fed a HFD for 12 wk and then injected with adenoviral sh-control or shMGAT1 via tail vein. After 1 wk with continuous high-fat feeding, mice were killed for analysis. As shown in Fig. 6 *A–C*, knockdown of hepatic MGAT1 significantly improved hepatic steatosis, without affecting the expression of PPARγ and its regulatory genes such as aP2/422 and CD36. Hepatic TG content was decreased by 25% after only 1 wk of MGAT1 knockdown (Fig. 6*D*), suggesting that MGAT1 expression plays a critical role in excessive hepatic lipid accumulation induced by high-fat feeding. Interestingly, hepatic MGAT1 knockdown also resulted in decreased body weight along with reduced liver weight, as well as improved glucose tolerance (Fig. 6 *E–G*). The biological parameters of these mice are shown in Fig. 6*H*, showing that blood glucose but not serum TG or LDL cholesterol was changed in this short period.

Similarly, the ob/ob mice that develop an obese phenotype with severe hepatic steatosis were injected with Ad-shMGAT1, showing dramatic improvement of fatty liver after 1 wk as shown

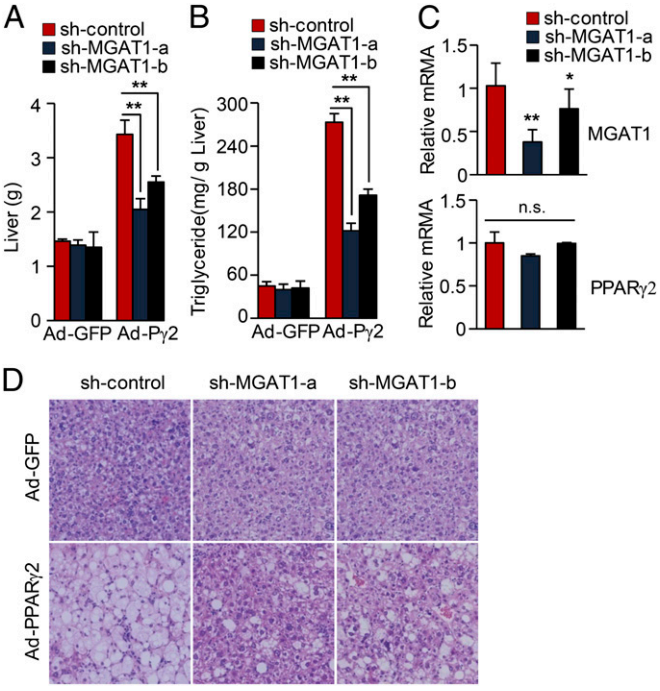


**Fig. 5.** Knockdown of MGAT1 expression improves hepatic steatosis in PPARγ-overexpressing liver. B6 mice were injected with either Ad-US (sh-control) or Ad-sh-MGAT1 along with Ad-GFP or Ad-PPARγ2 via tail vein. Two different shRNAs targeting MGAT1 cDNA were attempted, designated as sh-MGAT1-a and sh-MGAT1-b. (*A*) The liver weights and (*B*) TG contents were determined after 1 wk of viral injection. (*C*) Real-time PCR of the liver samples showed knockdown of MGAT1 expression. (*D*) H&E staining was performed after 1 wk of viral injections with liver sections. Data in *A–C* represent the mean ± SD; $n = 4$. $^*P < 0.05$, $^{**}P < 0.01$; n.s., not significant.

CELL BIOLOGY

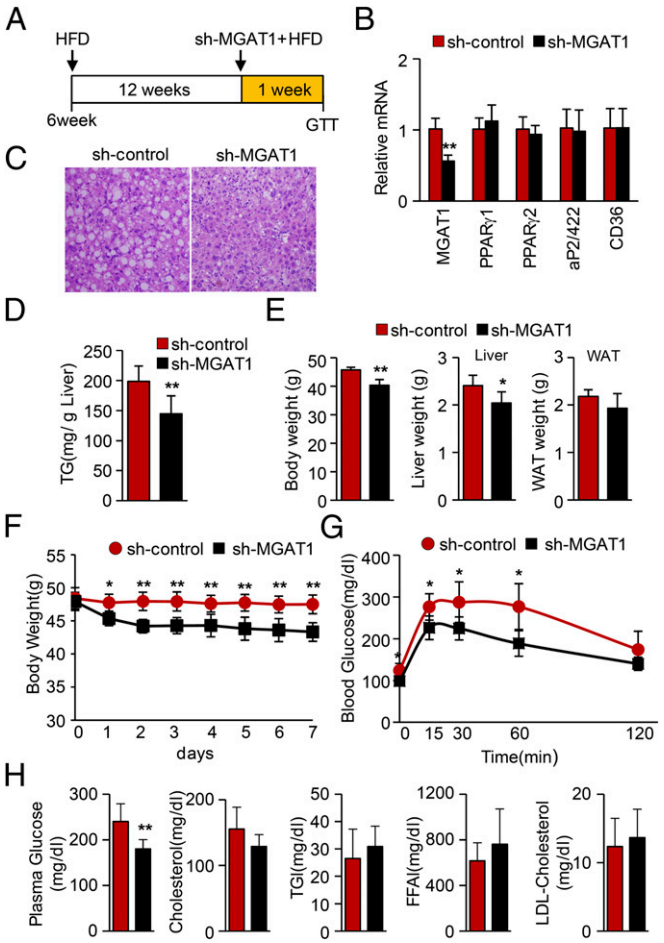


**Fig. 6.** Knockdown of MGAT1 improves hepatic steatosis in HFD-induced hepatic steatosis. (*A*) Six-week-old B6 mice were fed a HFD for 12 wk and then injected with adenoviral sh-control or sh-MGAT1 via tail vein. After 1 wk with continuous high-fat feeding, mice were killed. (*B*) Real-time PCR analysis showing efficient knockdown of MGAT1 in livers, without changes of PPARγ and its regulatory genes. (*C*) H&E staining of liver sections from mice. (*D*) Hepatic TG contents were determined. (*E*) Body weight, liver weights, and epididymal fat weights were determined. (*F*) Body weight changes were measured from the day of viral injection (day 0). (*G*) After 1 wk of viral injection, a glucose tolerance test was carried out. (*H*) Blood parameter after knockdown of MGAT1. Data in *B* and *D*–*H* represent the mean ± SD; $n = 6/6$. $^{*}P < 0.05$, $^{**}P < 0.01$.

by H&E staining (Fig. S7). The ob/ob mice treated by shMGAT1 also showed reduced body weight accompanied by significantly decreased epididymal fat content (Fig. S7 *A* and *C*). It is not clear whether the improvement of hepatic steatosis in high-fat–fed mice and ob/ob mice by MGAT1 knockdown is directly associated with body weight or systemic insulin resistance; however, these results suggest that the MGAT1 pathway induced by hepatic PPARγ is critically important in the development of hepatic steatosis during diet-induced obesity.

## Discussion

In this study, we report evidence for a role of PPARγ-regulated MGAT1 in hepatic steatosis. One of the critical findings of this study was that C3H mice do not express PPARγ and MGAT1 in the liver and are protected against hepatic steatosis while being fed a HFD. Importantly, because white adipose tissue of C3H mice expressed almost the same amount of PPARγ, the observed resistance to hepatic steatosis is considered liver specific and not the result of PPARγ function or expression in other tissues. Previously, C3H/HeJ mice with a loss-of-function mutation in the TLR4 gene (14) were reported to be DIO resistant on the basis of findings related to adipose tissue (19). However, C3H/HeN mice carry the wild-type TLR4 and are also reported to be to resistant to obesity-related disorders similar to their C3H/HeJ counterparts (20). This controversy might be due to a different interpretation of the results, because the phenotypes of both C3H mice are generally different from those of other DIO-prone mice. As we report in this study, both C3H strains became obese in response to HFD compared with B6 mice, but neither strain developed hepatic steatosis to the extent seen in B6 mice, suggesting that TLR4 is not sufficient to explain the accumulation of excessive lipids in the liver.

The fact that liver-specific inhibition of PPARγ confers resistance to hepatic steatosis suggests that PPARγ plays pivotal role in fatty liver, independent of the SREBP1c gene. ApoB/BATless mice do not show increased levels of hepatic SREBP1c, despite the presence of insulin resistance and hyperinsulinemia (21). SREBP1c gene deletion in mice results in a 50% decrease in fatty acid synthesis, indicating that SREBP1c activity alone is not sufficient to completely eliminate fatty acid synthesis (22). Furthermore, knockdown of PPARγ2 significantly decreased the liver TG content with a reduction in lipogenic genes in mice fed HFD, with no alteration of SREBP1c mRNA expression (23). We found that C3H mice lacking hepatic PPARγ also showed elevated SREBP1c levels with a HFD, similar to B6 mice, but C3H mice did not develop severe hepatic steatosis, suggesting that PPARγ rather than SREBP1c directly contributes to fatty liver in response to HFD.

In the present study, adenoviral overexpression of PPARγ2 resulted in marked induction of several PPARγ targets, including FSP27, aP2/422, CD36, and ADRP. TG accumulation by FSP27 and ADRP may occur through the TG protection from constitutive lipolysis (12, 24, 25). In addition, PPARγ regulates the genes related to TG synthesis. Of three identified MGAT enzymes (17, 26, 27), MGAT2 and MGAT3 are highly expressed in the small intestine, whereas MGAT1 mRNA was detected in stomach,

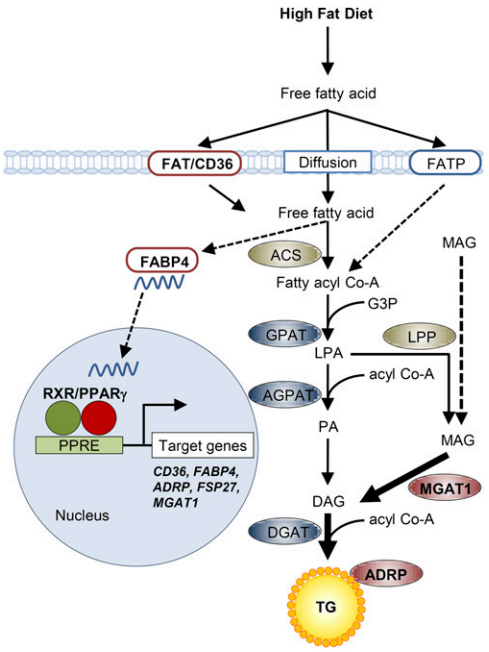


**Fig. 7.** A proposed model for the role of PPARγ and its regulation of target genes in hepatic steatosis. In diet-induced hepatic steatosis, increased activity of PPARγ and resulting increased MGAT1 expression enhance TG accumulation, regardless of fatty acid synthesis regulated by SREBP1c. ACS, acyl Co-A synthetase; DAG, diacylglycerol; G3P, glycerol-3-phosphate; GPAT, glycerol-3-phosphate acyltransferases; LPA, lysophosphatidic acid; LPP, lipid phosphate phosphatase, MAG, monoacylglycerol; PA, phosphatidic acid.

adipose tissue, and kidney. We showed that MGAT1 expression was very low in normal liver but was highly expressed in the fatty liver. We also demonstrate that the MGAT1 gene is directly regulated by PPARγ. This result is important because PPARγ may contribute to rapid TG incorporation via alternative pathways using increased MGAT1 enzyme. Indeed, we show that expression of adenoviral PPARγ in primary hepatocytes or mouse livers induced MGAT1 expression. Moreover, we observed the suppression of MGAT1 expression protected liver from fatty changes in three models: Ad-PPARγ-induced steatosis, 12-wk HFD-induced steatosis, and ob/ob mice with hepatic steatosis. It is likely that several PPARγ-regulated genes, such as aP2/422, CD36, and MGAT1, coordinate the enhanced TG accumulation in HFD-induced severe steatosis. However, blocking the MGAT1-associated alternative pathway might be an effective way to reduce the severity of PPARγ-induced hepatic steatosis in diet-induced obesity. It remains to be clarified by further study whether the inhibition of hepatic MGAT1 affects the body weight change or glucose tolerance.

On the basis of these data, we propose a model for the role of PPARγ in hepatic steatosis (Fig. 7). When plasma fatty acids are elevated either by diet or by release from adipose tissue, hepatic PPARγ is up-regulated and consequently activates fatty acid transporters and binding proteins, including CD36 and aP2/422. As a result, fatty acid uptake is markedly increased in hepatocytes. Fatty acids are then converted to fatty acyl CoA, which is ultimately esterified to TG. In addition, up-regulation of PPARγ in hepatocytes dramatically activates the MGAT pathway. Monoacylglycerol could also be generated from chylomicron remnants or hepatic TG, eventually increasing TG accumulation in the hepatocytes. In conclusion, PPARγ is responsible for activating the expression of genes involved in fatty acid uptake and TG synthesis, and the inhibition of PPARγ-induced MGAT1 for the alternative TG synthesis pathway would be one of the excellent therapeutic targets for hepatic steatosis.

## Materials and Methods

**Mice and Diet.** Male C57BL/6J, C3H/HeN, or C3H/HeJ mice were purchased from SLC. The animals were maintained in a temperature-controlled room (22 °C) on a 12:12-h light–dark cycle. Five- or 6-wk-old mice were fed a HFD (Research Diets) or a normal diet (Dyets) for up to 12 wk. The composition of the HFD we used was 60 kcal% fat containing 0 g/kg of corn starch, 125 g/kg of maltodextrin 10, 68.8 g/kg of sucrose, and 245 g/kg of lard. Body weight was measured once a week. All procedures were approved by the Committee on Animal Investigations of Yonsei University.

**Preparation of Recombinant Adenovirus.** Murine PPARγ2 and MGAT1 cDNAs were cloned into pcDNA3 vector or FLAG-tagged pcDNA3, respectively. Recombinant adenovirus expressing PPARγ2 and MGAT1-FLAG and ad-shRNA for MGAT1 were prepared. Recombinant adenovirus containing the GFP gene or Ad-US control RNAi was used as a control.

**Fatty Acid Uptake Assay.** Fatty acid uptake was measured with the QBT Fatty Acid Uptake Assay kit (Molecular Probes) according to the manufacturer's instructions. QBT Fatty Acid Uptake Assay stock solutions were dissolved completely by adding 10 mL of 1× HBSS buffer.

**In Vivo Effect of Adenovirus.** Seven-week-old male C57BL/6 mice and C3H/HeJ mice were injected with Ad-PPARγ2, Ad-MGAT1, or control recombinant adenovirus. Recombinant adenovirus ($2 \times 10^9$ pfu) was delivered by tail-vein injection to mice. Seven days after injection, mice were killed by terminal anesthesia. Similarly, ob/ob mice were used for the adenoviral injection via tail veins as described.

**Immunofluorescence.** Cells were cultured in 12 wells on glass coverslips and fixed in MeOH/acetone (1:1) at −20 °C for 30 min and blocked with 3% (wt/vol) BSA in PBS for 1 h. Cells were incubated for 2 h at room temperature (RT) with primary antibodies. Cells were washed and incubated with Alexa488- or Alexa555-conjugated secondary antibodies (Invitrogen) for 1 h at RT. Nuclei were revealed with DAPI staining. Confocal scanning was performed on an LSM700 scanning microscope (Carl Zeiss).

**Statistical Analysis.** All results are expressed as mean ± SEM. Statistical comparisons of groups were made using an unpaired Student's *t* test and two-way ANOVA.

For full details of all methods, please refer to *SI Materials and Methods*.

**ACKNOWLEDGMENTS.** We thank Dr. Eun Jik Lee (Yonsei University College of Medicine) and Dr. Seung-Hoi Koo (Sungkyunkwan University School of Medicine) for providing the adenoviral vector. This work was supported by National Research Foundation of Korea Grants 2011-0030711 and 2011-0015665, and World Class University (WCU) Grant R31-10086, funded by the Ministry of Education, Science and Technology (MEST) of the Korean government.

1. Marchesini G, et al. (2003) Nonalcoholic fatty liver, steatohepatitis, and the metabolic syndrome. *Hepatology* 37:917–923.
2. Reaven GM (1988) Banting lecture 1988. Role of insulin resistance in human disease. *Diabetes* 37:1595–1607.
3. Fabbrini E, Sullivan S, Klein S (2010) Obesity and nonalcoholic fatty liver disease: Biochemical, metabolic, and clinical implications. *Hepatology* 51:679–689.
4. Postic C, Girard J (2008) Contribution of de novo fatty acid synthesis to hepatic steatosis and insulin resistance: Lessons from genetically engineered mice. *J Clin Invest* 118:829–838.
5. Towle HC (2005) Glucose as a regulator of eukaryotic gene transcription. *Trends Endocrinol Metab* 16:489–494.
6. Semple RK, Chatterjee VK, O'Rahilly S (2006) PPAR gamma and human metabolic disease. *J Clin Invest* 116:581–589.
7. Rahimian R, et al. (2001) Hepatic over-expression of peroxisome proliferator activated receptor gamma2 in the ob/ob mouse model of non-insulin dependent diabetes mellitus. *Mol Cell Biochem* 224:29–37.
8. Vidal-Puig A, et al. (1996) Regulation of PPAR gamma gene expression by nutrition and obesity in rodents. *J Clin Invest* 97:2553–2561.
9. Yamauchi T, et al. (2001) Inhibition of RXR and PPARgamma ameliorates diet-induced obesity and type 2 diabetes. *J Clin Invest* 108:1001–1013.
10. Matsusue K, et al. (2003) Liver-specific disruption of PPARgamma in leptin-deficient mice improves fatty liver but aggravates diabetic phenotypes. *J Clin Invest* 111: 737–747.
11. Yu S, et al. (2003) Adipocyte-specific gene expression and adipogenic steatosis in the mouse liver due to peroxisome proliferator-activated receptor gamma1 (PPARgamma1) overexpression. *J Biol Chem* 278:498–505.
12. Schadinger SE, Bucher NL, Schreiber BM, Farmer SR (2005) PPARgamma2 regulates lipogenesis and lipid accumulation in steatotic hepatocytes. *Am J Physiol Endocrinol Metab* 288:E1195–E1205.
13. Poltorak A, et al. (1998) Defective LPS signaling in C3H/HeJ and C57BL/10ScCr mice: Mutations in Tlr4 gene. *Science* 282:2085–2088.
14. Tsukumo DM, et al. (2007) Loss-of-function mutation in Toll-like receptor 4 prevents diet-induced obesity and insulin resistance. *Diabetes* 56:1986–1998.
15. Liao J, Sportsman R, Harris J, Stahl A (2005) Real-time quantification of fatty acid uptake using a novel fluorescence assay. *J Lipid Res* 46:597–602.
16. Yen CL, Stone SJ, Cases S, Zhou P, Farese RV, Jr. (2002) Identification of a gene encoding MGAT1, a monoacylglycerol acyltransferase. *Proc Natl Acad Sci USA* 99:8512–8517.
17. Cortés VA, et al. (2009) Molecular mechanisms of hepatic steatosis and insulin resistance in the AGPAT2-deficient mouse model of congenital generalized lipodystrophy. *Cell Metab* 9:165–176.
18. West DB, Boozer CN, Moody DL, Atkinson RL (1992) Dietary obesity in nine inbred mouse strains. *Am J Physiol* 262:R1025–R1032.
19. Poggi M, et al. (2007) C3H/HeJ mice carrying a toll-like receptor 4 mutation are protected against the development of insulin resistance in white adipose tissue in response to a high-fat diet. *Diabetologia* 50:1267–1276.
20. Hwang IK, et al. (2008) Strain-specific differences in cell proliferation and differentiation in the dentate gyrus of C57BL/6N and C3H/HeN mice fed a high fat diet. *Brain Res* 1241:1–6.
21. Zhang YL, et al. (2006) Aberrant hepatic expression of PPARgamma2 stimulates hepatic lipogenesis in a mouse model of obesity, insulin resistance, dyslipidemia, and hepatic steatosis. *J Biol Chem* 281:37603–37615.
22. Liang G, et al. (2002) Diminished hepatic response to fasting/refeeding and liver X receptor agonists in mice with selective deficiency of sterol regulatory element-binding protein-1c. *J Biol Chem* 277:9520–9528.
23. Kim JK, et al. (2001) Tissue-specific overexpression of lipoprotein lipase causes tissue-specific insulin resistance. *Proc Natl Acad Sci USA* 98:7522–7527.
24. Matsusue K, et al. (2008) Hepatic steatosis in leptin-deficient mice is promoted by the PPARgamma target gene Fsp27. *Cell Metab* 7:302–311.
25. Brasaemle DL, et al. (2000) Perilipin A increases triacylglycerol storage by decreasing the rate of triacylglycerol hydrolysis. *J Biol Chem* 275:38486–38493.
26. Cao J, Lockwood J, Burn P, Shi Y (2003) Cloning and functional characterization of a mouse intestinal acyl-CoA:monoacylglycerol acyltransferase, MGAT2. *J Biol Chem* 278:13860–13866.
27. Cheng D, et al. (2003) Identification of acyl coenzyme A:monoacylglycerol acyltransferase 3, an intestinal specific enzyme implicated in dietary fat absorption. *J Biol Chem* 278:13611–13614.